Electronic Supplementary Material (ESI) for Journal of Materials Chemistry A.

Supporting Information

A Novel Self-catalytic Cooperative Multiple Dynamic Moiety: Towards Rigid and Tough but More Healable Polymer Networks

Maoyu Yang, Xili Lu,* Zhanhua Wang, Guoxia Fei, Hesheng Xia*

State Key Laboratory of Polymer Materials Engineering, Polymer Research Institute, Sichuan University, Chengdu, 610065, China.

*Corresponding author. *E*-mail: xililu@scu.edu.cn; xiahs@scu.edu.cn

1. Experimental Section

1.1 Materials

O,O'-bis(2-aminopropyl) polypropylene glycol-block-polyethylene glycol-block-polypropylene glycol 500 (ED600, Aldrich, Mr ≈ 600 g mol^{-1}), dimethyl 2,6-Pyridinedicarboxylate (DPDC, Adamas, >98 %), hydrazine monohydrate ($N_2H_4 \cdot H_2O$, Adamas, 80% Aq.*), isophorone diisocyanate (IPDI, Adamas, >99 %), 1-Butyl Isocyanate (1-BI, TCI, >98 %), hexamethylene diisocyanate trimer (tri-HDI, Bayer, Desmodur N3300), Benzylamine (BA, TCI, >99 %), Anhydrous zinc chloride ($ZnCl_2$, TCI, >98 %), N,N-dimethylformamide (DMF, Adamas, ≥99.5 %, water ≤50 ppm), tetrahydrofuran (THF, Adamas, ≥99.5 %, water ≤50 ppm). All the solvents and reagents were obtained from commercial suppliers and used without further purification.

1.2 Synthetic Procedures

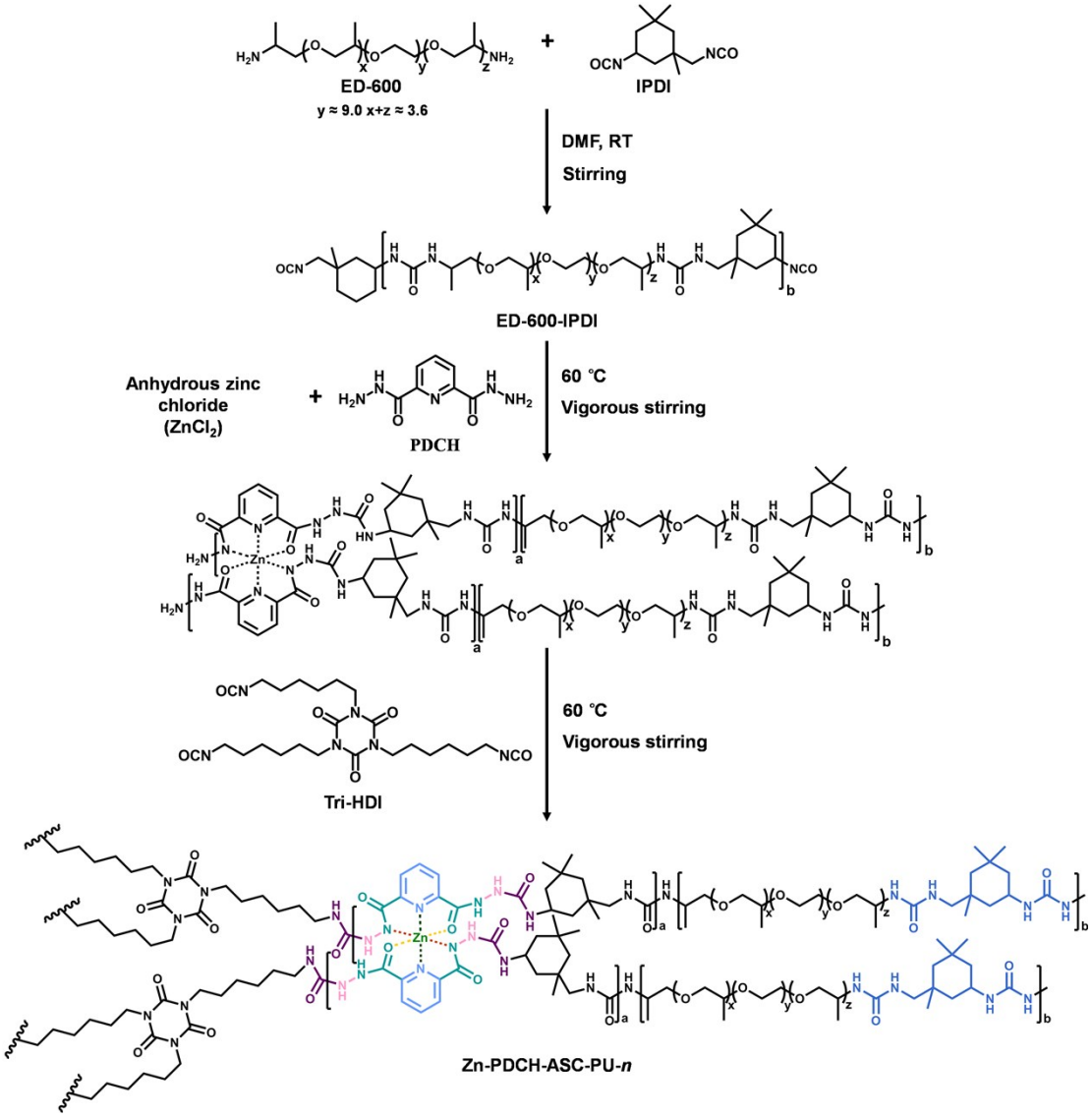

Scheme S1. Synthetic routes for cross-linked Zn-PDCH-ASC-PU-n.

1.2.1 Synthesis of Pyridine-2,6-dicarbobohydrazide (PDCH)

A suspension of dimethyl 2,6-Pyridinedicarboxylate (DPDC, 19.52 g, 100 mmol) in 200 mL ethanol was charged to a 500 mL flask with a magnetic stir bar at 80 °C. Hydrazine hydrate ($N_2H_4 \cdot H_2O$, 10 g, 200 mmol) was added into the solution via syringe under vigorous stirring. The suspension turned into a clear solution within a few seconds,

after that the product precipitated from the solution immediately. The reaction was allowed to proceed for 12 h. The precipitate was collected by vacuum filtration and washed with cold ethanol. The resulting powder was vacuum dried under 60 °C for 24 h to obtain the purified pyridine-2,6-dicarbohydrazide (PDCH, 17.41 g, ~89.2 %) as a white solid. The ^{1}H NMR and ^{13}C NMR spectra are shown in Fig. S14 and S15 respectively. ^{1}H NMR (400 MHz, DMSO-d_6, 298 K) δ (ppm): 10.64 (s, 2 H), 8.13 (s, 3 H), 4.63 (br s, 4 H). ^{13}C NMR (100 MHz, DMSO-d_6, 298 K) δ (ppm): 162.40, 148.89, 139.81, 124.17.

1.2.2 Synthesis of N'²,N'⁶-Bis(n-butylhydrazine)pyridine-2,6-dicarbohydrazide (BI-PDCH-BI)

A suspension of pyridine-2,6-dicarbohydrazide (PDCH, 1.95 g, 10 mmol) in 20 mL tetrahydrofuran (THF) was charged to a 50 mL flask with a magnetic stir bar at 40 °C. 1-butyl isocyanate (1-BI, 2.97 g, 30 mmol) was added into the solution via dropper under vigorous stirring. The reaction was allowed to proceed for 12 h. After that the product was collected by vacuum filtration and washed with cold THF. The resulting powder was vacuum dried under 60 °C for 24 h to obtain the purified BI-PDCH-BI (3.08 g, 86.3%) as a white solid. The ^{1}H NMR and ^{13}C NMR spectra are shown in Fig. S16 and S17 respectively. ^{1}H NMR (400 MHz, DMSO-d_6, 298 K) δ (ppm): 10.91 (s, 2 H), 8.21 (s, 3 H), 7.96 (s, 2 H), 6.50 (s, 2 H), 3.03 (q, J = 6.4 Hz, 4 H), 1.4 –1.35 (m, 4 H), 1.33–1.24 (m, 4 H), 0.88 (t, J = 7.2 Hz, 6 H). ^{13}C NMR (100 MHz, DMSO-d_6, 298 K) δ (ppm): 163.32, 158.60, 148.58, 139.91, 125.19, 39.36, 32.44, 19.91, 14.20.

1.2.3 Synthesis of Zn-BI-PDCH-PU-Complex

A solution of $ZnCl_2$ (136 mg, 1.00 mmol) in 1 mL of methanol was slowly added with stirring to a solution of BI-PDCH-BI (826 mg, 2.10 mmol) in 20 mL methanol. The resulting light-yellow solution was stirred for 12 h at room temperature. Then the solution was evaporated under reduced pressure and the residue was washed with diethyl ether (3×50 mL) to afford the purified Zn-BI-PDCH-BI-Complex (752 mg, 81.5 %) as a yellow solid.

1.2.4 Synthesis of 1-Benzyl-3-butylurea (BA-BI)

BA-BI was synthesized using similar procedures as BI-PDCH-BI via the reaction of Benzylamine (BA) with 1-butyl isocyanate (1-BI), affording a white solid (yield ~84.2 %). The ^{1}H NMR and ^{13}C NMR spectra are shown in Fig. S18 and S19 respectively. ^{1}H NMR (400 MHz, DMSO-d_6, 298 K) δ (ppm): 7.32–7.19 (m, 5 H), 6.24 (s, 1H), 5.88 (s, 1H), 4.19 (d, J = 5.6 Hz, 2 H), 3.00 (q, J = 6.4 Hz 2 H), 1.39–1.31 (m, 2 H), 1.29–1.22 (m, 2 H), 0.87 (t, J = 7.2 Hz, 3 H). ^{13}C NMR (100 MHz, DMSO-d_6, 298 K) δ (ppm): 158.54, 141.51, 128.65, 127.44, 126.96, 43.35, 39.46, 32.64, 20.00, 14.19.

1.2.5 Synthesis of Zn-PDCH-ASC-PU-n and the control sample PDCH-ASC-PU

The Zn-PDCH-ASC-PU-n was synthesized according to the above routes. Typically, for Zn-PDCH-ASC-PU-0.5, the precursor ED600-IPDI was synthesized by the reaction of ED600 (6.00 g, 10 mmol) and IPDI (2.96 g, 13.33 mmol) with a 3 : 4 molar ratio in anhydrous DMF (20 mL) at room temperature for 3 h. Then, a stoichiometric amount of PDCH (0.94 g, 4.81 mmol) and anhydrous $ZnCl_2$ (0.39 g, 2.41 mmol) were added into the reaction at 60 °C under vigorous stirring for 12 h to obtain supramolecular PU networks containing Zn-PDCH coordinations and ASC moieties. After that, the crosslinker hexamethylene diisocyanate trimer (tri-HDI) (0.50 g, 0.99 mmol) was added into the supramolecule solution under heating at 60 °C for 1 h. The resulting mixture was degassed under reduced pressure and cast into a polytetrafluoroethylene (PTFE) mold measuring 10 cm (L) × 10 cm (W) × 5.0 mm (D). The mold was put into an oven at 40 °C under an anhydrous atmosphere, and the temperature was gradually increased to 80 °C for removing the solvent and allowing the completion of the reaction. The polymer Zn-PDCH-ASC-PU-0.5 was further dried under vacuum at 85 °C for 48 h to obtain a light-yellow transparent sheet with a dimension of 10cm (L) × 10 cm (W) × 0.4-0.7 mm (T), which was kept in a desiccator for further measurements. Zn-PDCH-ASC-PU-0.25 and Zn-PDCH-ASC-PU-1 were obtained using the same method by adding different amount of $ZnCl_2$. The colorless transparent control sample PDCH-ASC-PU without Zn-PDCH coordinations was synthesized without adding anhydrous $ZnCl_2$ using similar procedures.

1.3 Characterizations

1.3.1 General characterization

Flourier transformed infrared spectroscopy (FTIR) analysis of the samples was performed on a Nicolet 560 FTIR

spectrometer; Nuclear magnetic resonance (NMR) experiments were conducted by Bruker ARX-400 at 400 MHz with DMSO-d6 as solvent. The morphology of Zn-PDCH-ASC-PU-0.5 was observed on a FEI Tecnai G2 F20 S-TWIN transmission electron microscope. Mechanical tensile-stress experiments were conducted on an Instron 5567 machine (USA) at room temperature (~25 °C) with a strain rate of 50 mm min^{-1}, and dog bone shaped samples [0.4~0.7 mm (T) × 2 mm (W) × 35 mm (L)] and a gauge length of 15 mm were used. At least three samples of each loading fraction were tested and the reported results were average values. Thermogravimetric analysis (TGA) experiments were performed on a NETZSCH TG 209 instrument at a linear heating rate of 10 °C min^{-1} from 30 to 800 °C under a nitrogen atmosphere. UV-Vis absorption spectra were recorded on a Cary 60 spectrometer (Agilent Technologies). Dynamic mechanical thermal analysis (DMTA) was carried out on a DMA Q800 apparatus (TA Instrument) in a tension film mode, and the rectangular geometry samples (ca. 0.5 mm (T) × 3 mm (W) × 20 mm (L)) were measured with a gauge length of ~8 mm from -50 °C to 180 °C at a heating rate of 3 °C min^{-1}, under a strain of 0.1 % and frequency of 1 Hz. Both stress-relaxation analysis (SRA) were performed using a tensile mode on a DMA Q800 apparatus (TA Instrument), and rectangular samples were utilized (ca. 0.5 mm (T) × 3 mm (W) × 20 mm (L) and a gauge length of ~8 mm). For the SRA, the built-in stress relaxation mode was used. Samples were equilibrated at a set temperature for 5 min, and then subjected to a constant strain of 10 %. The stress decay over time was monitored.

1.3.2 UV-Vis titration of $ZnCl_2$ into PDCH-ASC-PU solution

A small volume of anhydrous $ZnCl_2$ in methanol (1 mmol L^{-1}) was added to a diluted solution of PDCH-ASC-PU in 6 mL DMF (0.1 mg mL^{-1}), which was prepared by heating the dynamic polymer network in DMF at 120 °C. Each time the volume of the $ZnCl_2$ solution is 20 μL. After addition, the mixture was stirred for 1 min to ensure the complete coordination before UV-Vis recording.

1.3.3 Noda's rule for the generalized 2D correlation spectra

If the correlation intensity $\Phi(\nu_1, \nu_2)$ in synchronous spectra has the same sign ("+" or "−") as the correlation peak $\Psi(\nu_1, \nu_2)$ in asynchronous spectra, then the movement of band ν_1 is prior to or earlier than that of band ν_2, and vice versa. Besides, if the correlation in synchronous spectra is not zero (or blank), but zero in asynchronous one, then the movements of bands at ν_1 and ν_2 are simultaneous.

Noda's rules are summarized as follows:

(1) If $\Phi(\nu_1, \nu_2) > 0$, $\Psi(\nu_1, \nu_2) > 0$ or $\Phi(\nu_1, \nu_2) < 0$, $\Psi(\nu_1, \nu_2) < 0$, then the movement of ν_1 is before than that of ν_2.

(2) If $\Phi(\nu_1, \nu_2) > 0$, $\Psi(\nu_1, \nu_2) < 0$ or $\Phi(\nu_1, \nu_2) < 0$, $\Psi(\nu_1, \nu_2) > 0$, then the movement of ν_1 is after than that of ν_2.

(3) If $\Phi(\nu_1, \nu_2) > 0$, $\Psi(\nu_1, \nu_2) = 0$ or $\Phi(\nu_1, \nu_2) < 0$, $\Psi(\nu_1, \nu_2) = 0$, then the movements of ν_1 and ν_2 are simultaneous.

$\Phi(\nu_1, \nu_2)$ and $\Psi(\nu_1, \nu_2)$ represent the correlation peaks in synchronous and asynchronous spectra, respectively.

1.3.4 Stress relaxation analysis

For the stress relaxation analysis, the rectangular samples were maintained under a strain of 10 %, and the decay of the stress over time was monitored at different temperatures. The relaxation modulus (E) was normalized by initial value (E_0), and the relaxation time τ should be determined as the time when $E/E_0 = 1/e$. The stress-relaxation properties conform to the Maxwell model, and the relaxation modulus (E) has an exponential relationship with time (t):

$$E(t) = E_0 exp^{(-t/\tau)} \quad \text{(S1)}$$

Moreover, the relationship of the relaxation time τ and temperature follows the Arrhenius equation:

$$\tau(T) = \tau_0 exp^{\left(E_{a,r}/RT\right)} \quad \text{(S2)}$$

Where $\tau(T)$ relaxation time at temperature T, τ_0 = relaxation time at infinite temperature, $E_{a,r}$ = relaxation activation energy, R = universal gas constant, and T = absolute temperature.

1.3.5 Reprocessing of the materials

The PDCH-ASC-PU and Zn-PDCH-ASC-PU-0.5 were cut into small pieces, and washed with dichloromethane (DCM) to remove surface contaminants, following by vacuum drying. The cleaned polymer granules were placed into a square metal mold [ca. 0.5 mm (D) × 50 mm (L) × 50 mm (W)] between two polyimide films, and then hot-pressed under 10 MPa at various temperatures and time durations. After that, the mold was cooled to room temperature.

2. Supplementary Figures

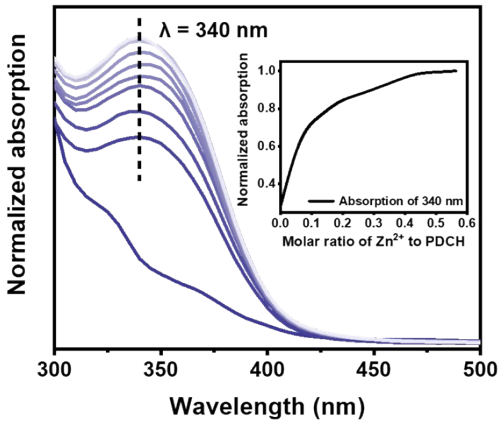

Fig. S1 UV-Vis spectra change with the titration of a solution of anhydrous $ZnCl_2$ (0.01 mol L^{-1}) in methanol into the diluted PDCH-ASC-PU solution (0.1 mg mL^{-1}) in DMF; inset is the absorption at defined wavelength (λ = 340 nm) changes with the ratio of Zn^{2+} to PDCH.

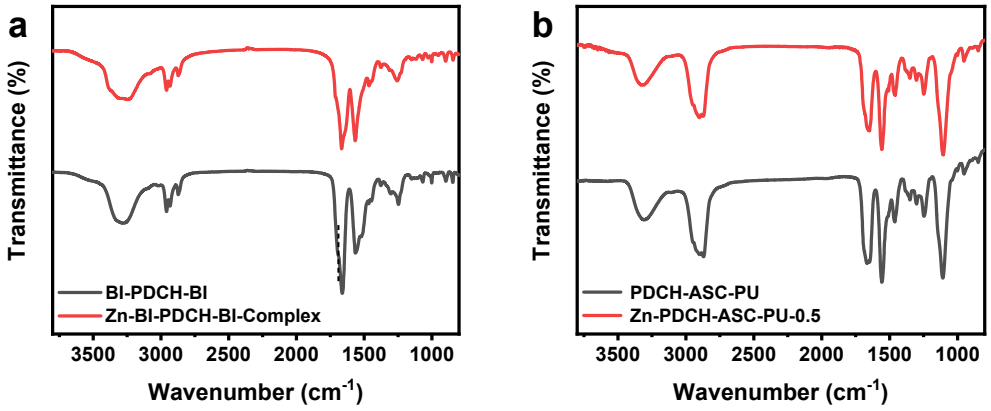

Fig. S2 FTIR spectra of (a) small model compounds BI-PDCH-BI/Zn-BI-PDCH-BI-Complex and (b) polymer networks PDCH-ASC-PU/Zn-PDCH-ASC-PU-0.5 in the range of 3800-800 cm^{-1}.

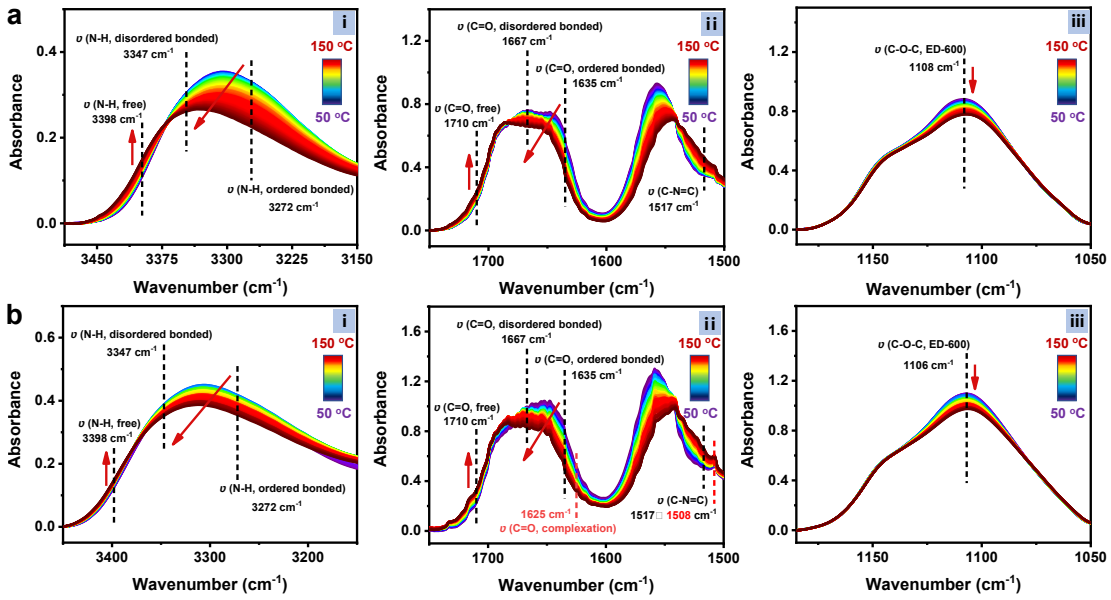

Fig. S3 The in-situ FTIR spectra of (a) PDCH-ASC-PU and (b) Zn-PDCH-ASC-PU-0.5 upon heating from 50 °C to 150 °C, (i) 3480-3120 cm^{-1}, (ii) 1750-1400 cm^{-1}, (iii) 1180-1050 cm^{-1}.

***In-situ* FTIR study of the materials**

In Fig. S3 a-i and b-i, the band at 3398 cm^{-1} is assigned to the N-H stretching of "free" N-H groups.[1] The band at 3347 cm^{-1} is attributed to the N-H stretching of disordered hydrogen-bonded N-H groups, and 3272 cm^{-1} is the N-H stretching of the ordered hydrogen-bonded N-H groups.[1-3] It can be observed that, the intensity of the band at 3398 cm^{-1} enhances as the temperature increases, indicating the generation of "free" N-H groups both in PDCH-ASC-PU and Zn-PDCH-ASC-PU-0.5 upon heating (50~150 °C). At the same time, partial peaks at 3272 cm^{-1} gradually moves to the high wavenumber (3347 cm^{-1}), accompanying by a decrease of peak width and peak intensity. This shows that the ordered hydrogen-bonded N-H groups are gradually transformed into the disordered hydrogen-bonded N-H groups.

In Fig. S3 a-ii and b-ii, the bands of 1710, 1667, 1635 and 1625 cm^{-1} are assigned to the amide I bands.[1] The peak at 1710 cm^{-1} is attributed to the C=O stretching of "free" C=O groups; the band at 1667 cm^{-1} is the C=O stretching of the disordered hydrogen-bonded C=O groups, and 1635 cm^{-1} is assigned to the C=O stretching of the ordered hydrogen-bonded C=O groups.[1-3] As the temperature increases (50~150 °C), the band intensity of 1710 cm^{-1} raises, and those of 1667 cm^{-1} and 1635 cm^{-1} gradually decreases. Meanwhile, partial band positions moving from 1635 cm^{-1} to 1667 cm^{-1} is also observed upon heating (50~150 °C). This clearly reveals the hydrogen bonds generation from "free" C=O groups and the transformation from the ordered hydrogen-bonded C=O groups to the disordered hydrogen-bonded C=O groups. Note that the band intensity of 1625 cm^{-1} (Fig. S3 b-ii) which is assigned to the C=O stretching of the coordination-bonded C=O groups gradually reduces upon heating (50~150 °C), indicating the decomposition of the coordination complex.[4]

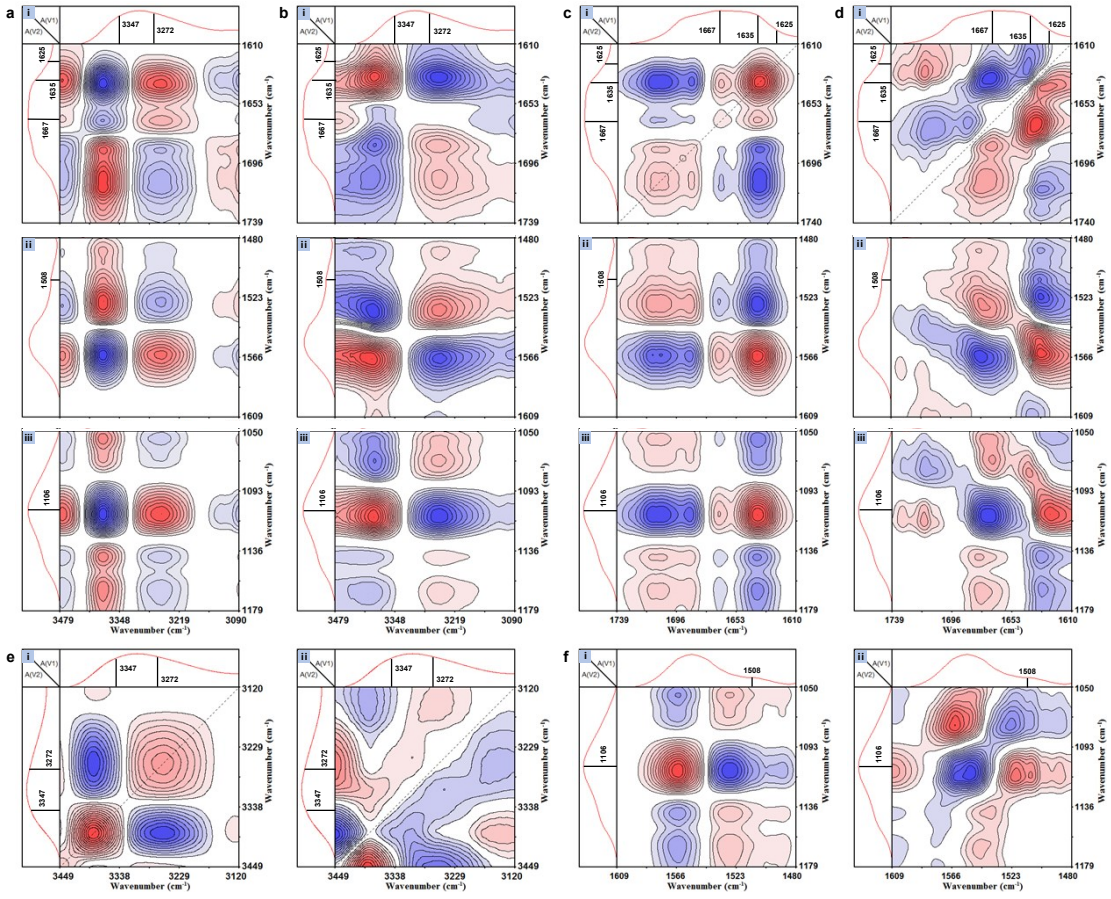

Fig. S4 Generalized synchronous (a, c, e-i and f-i) and asynchronous (b, d, e-ii and f-ii) 2D correlation spectra of Zn-PDCH-ASC-PU-0.5 calculated from the temperature-dependent FTIR spectra in the regions of 3479-3090 cm^{-1} vs. 1739-1610 cm^{-1} (a-i and b-i), 3479-3090 cm^{-1} vs. 1609-1480 cm^{-1} (a-ii and b-ii), 3479-3090 cm^{-1} vs. 1179-1050 cm^{-1} (a-iii and b-iii), 1739-1610 cm^{-1} vs. 1740-1610 cm^{-1} (c-i and d-i), 1739-1610 cm^{-1} vs. 1609-1480 cm^{-1} (c-ii and d-ii), 1739-1610 cm^{-1} vs. 1179-1050 cm^{-1} (c-iii and d-iii), 1609-1480 cm^{-1} vs. 1179-1050 cm^{-1} (e-i and e-ii) and 3449-3120 cm^{-1} vs. 3449-3120 cm^{-1} (f-i and f-ii). The red and blue areas represent the positive "+" and negative "–" correlation intensity, respectively.

2D Correlation analysis of the materials

The signs ("+" or "−") of the cross correlation peaks (v_1, v_2) in synchronous and asynchronous spectra were obtained from Fig. S4, as summarized in Table S2. According to Noda's rules, the sequential order of the bands of ν(1106 cm^{-1}, C-O-C, ED-600), ν(1508 cm^{-1}, C=N-C, coordination), ν(1625 cm^{-1}, C=O, coordination), ν(1635 cm^{-1}, C=O, ordered bonded), ν(1667 cm^{-1}, C=O, disordered bonded), ν(3347 cm^{-1}, N-H, disordered bonded), ν(3272 cm^{-1}, N-H, ordered bonded) could be judged from Table S2. For example, Φ(3347 cm^{-1}, 3272 cm^{-1}) < 0, Ψ(3347 cm^{-1}, 3272 cm^{-1}) > 0, it can be concluded that 3347 cm^{-1} ← 3272 cm^{-1}(the symbol "←" means "after", and "→" means "before", the movement of the band at 3347 cm^{-1} comes after that of the band at 3272 cm^{-1}). Similarly, we can obtain 3347 cm^{-1} → 1667 cm^{-1} and further 3272 cm^{-1} → 3347 cm^{-1} → 1667 cm^{-1}. By using the same method, we can finally infer that 1625 cm^{-1} → 1635 cm^{-1} → 1106 cm^{-1} → 1508 cm^{-1} → 3272 cm^{-1} → 3347 cm^{-1} → 1667 cm^{-1}. The corresponding sequential order of groups' movement is ν(C=O, coordination) → ν(C=O, ordered bonded) → ν(C-O-C, ED-600) → ν(C=N-C, coordination) → ν(N-H, ordered bonded) → ν(N-H, disordered bonded) → ν(C=O, disordered bonded).□□□□□□

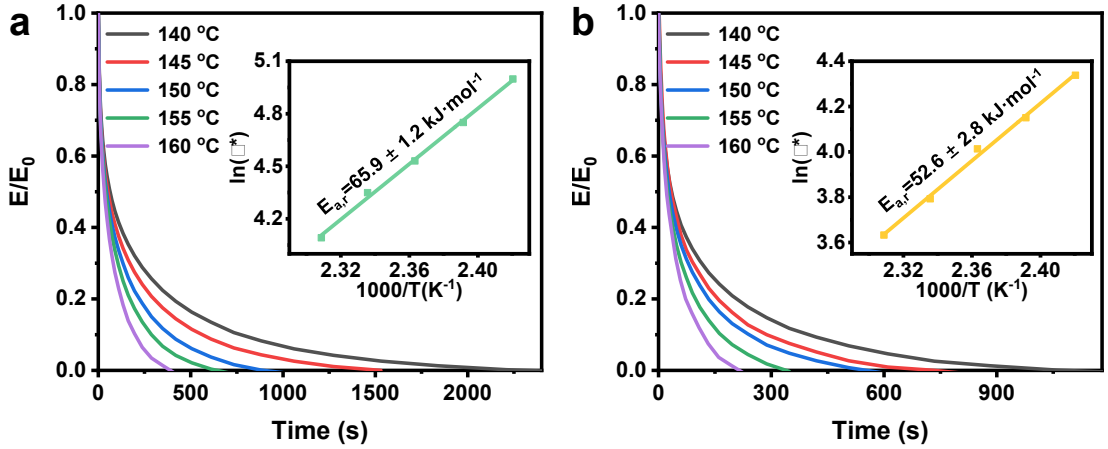

Fig. S5 Stress relaxation analysis of (a) Zn-PDCH-ASC-PU-0.25 and (b) Zn-PDCH-ASC-PU-1 at various temperatures. Inset diagram is the fitted line of the relaxation times according to the Arrhenius equation.

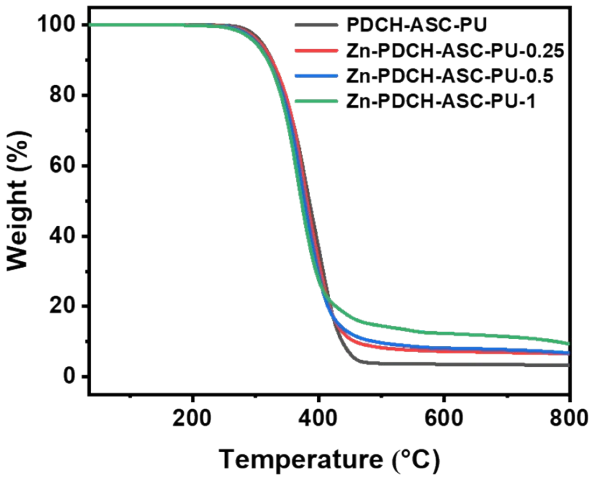

Fig. S6 TGA traces of PDCH-ASC-PU and Zn-PDCH-ASC-PU-n containing different amount of Zn^{2+} ions under nitrogen atmosphere at a heating rate of 10 °C min^{-1}.

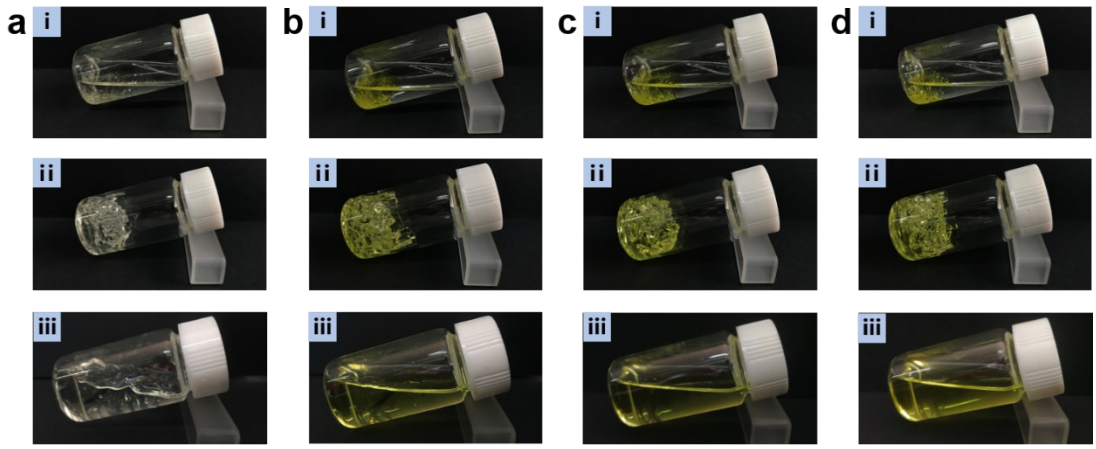

Fig. S7 Photographs showing polymer granules of (a) PDCH-ASC-PU, (b) Zn-PDCH-ASC-PU-0.25, (c) Zn-PDCH-ASC-PU-0.5 and (d) Zn-PDCH-ASC-PU-1 (i) being immersed in DMF at RT before swelling, (ii) after swelling for 24 h, and (iii) after adding 5 mL DMF and heating at 120 °C for 2 h.

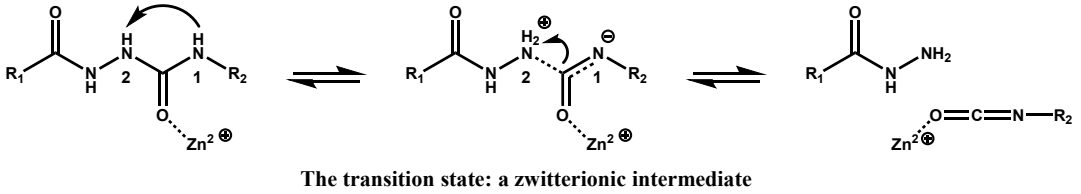

Scheme S2. Schematic illustration of the mechanism of the Zn-catalyzed reversible dissociation and reformation of the ASC moiety.

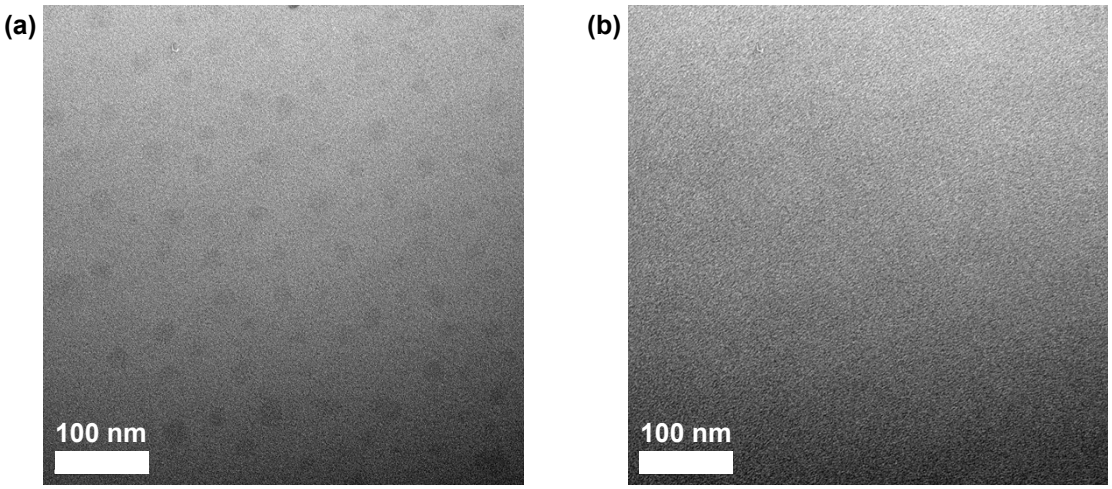

Fig. S8 TEM image of (a) Zn-PDCH-ASC-PU-0.5 and (b) PDCH-ASC-PU.

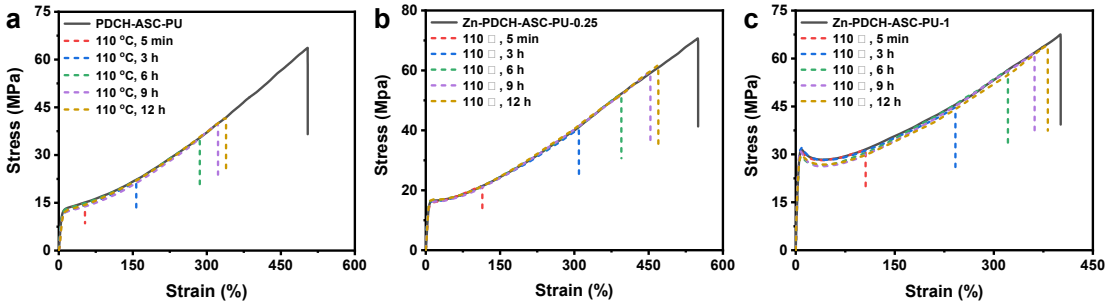

Fig. S9 Stress and strain curves of the healed (a) PDCH-ASC-PU, (b) Zn-PDCH-ASC-PU-0.25 and (c) Zn-PDCH-ASC-PU-1 under different repairing time at 110 °C.

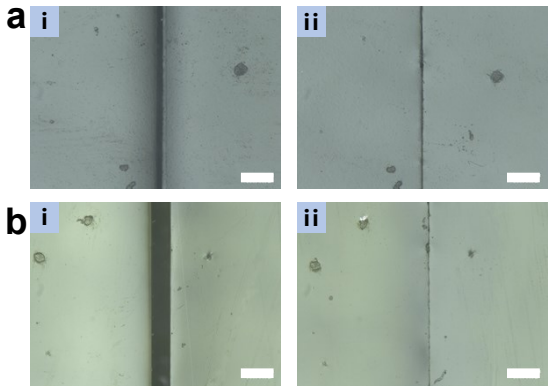

Fig. S10 Optical microscopy images of the scratched (a) PDCH-ASC-PU and (b) Zn-PDCH-ASC-PU-0.5 film before (i) and after (ii) self-healing at 110 °C for 5 min. Scale bar: 100 μm.

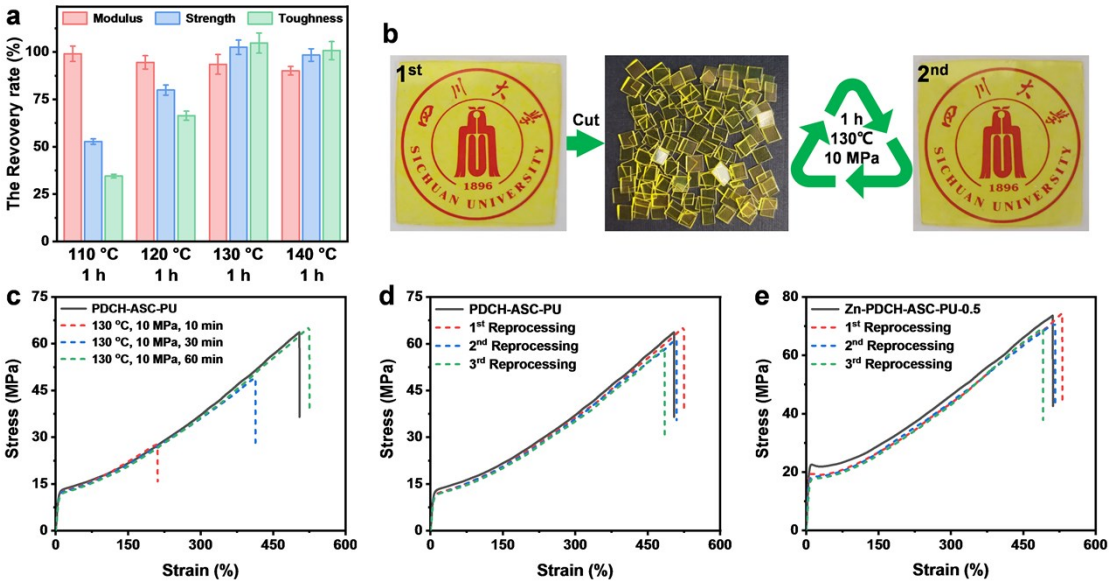

Fig. S11 (a) The recovery rate of Young's modulus (red), tensile strength (blue) and tensile toughness (green) after remolding at different temperature. (b) Photographs showing the reprocessing of Zn-PDCH-ASC-PU-0.5. (c) Stress-strain curves of the recycled PDCH-ASC-PU samples after hot-pressing for different time durations. Stress-strain curves of recycled (d) PDCH-ASC-PU and (e) Zn-PDCH-ASC-PU-0.5 samples for the first, second and third cycles of reprocessing.

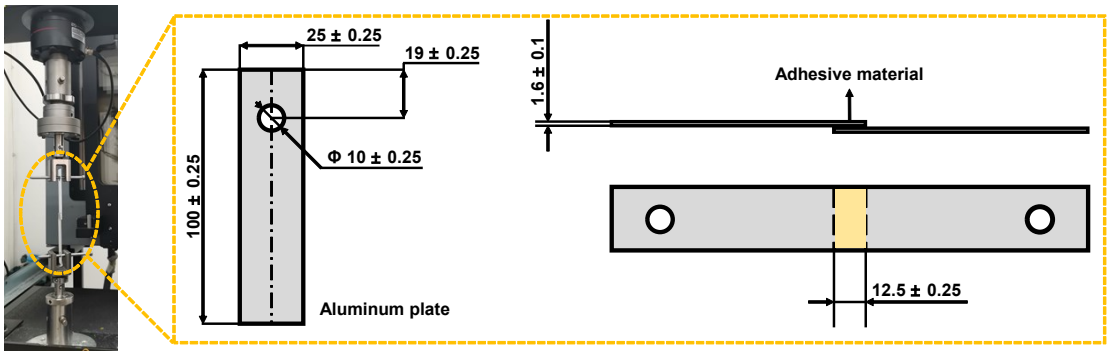

Fig. S12 Schematic illustration of the test standard of lap shear adhesion experiment.

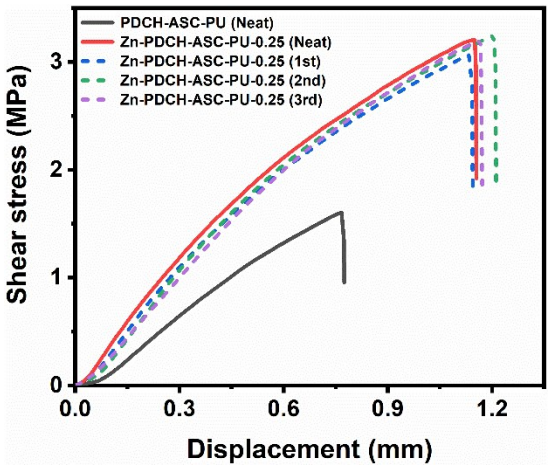

Fig. S13 The stress-displacement curves of the lap shear adhesion tests for Zn-PDCH-ASC-PU-n and PDCH-ASC-PU.

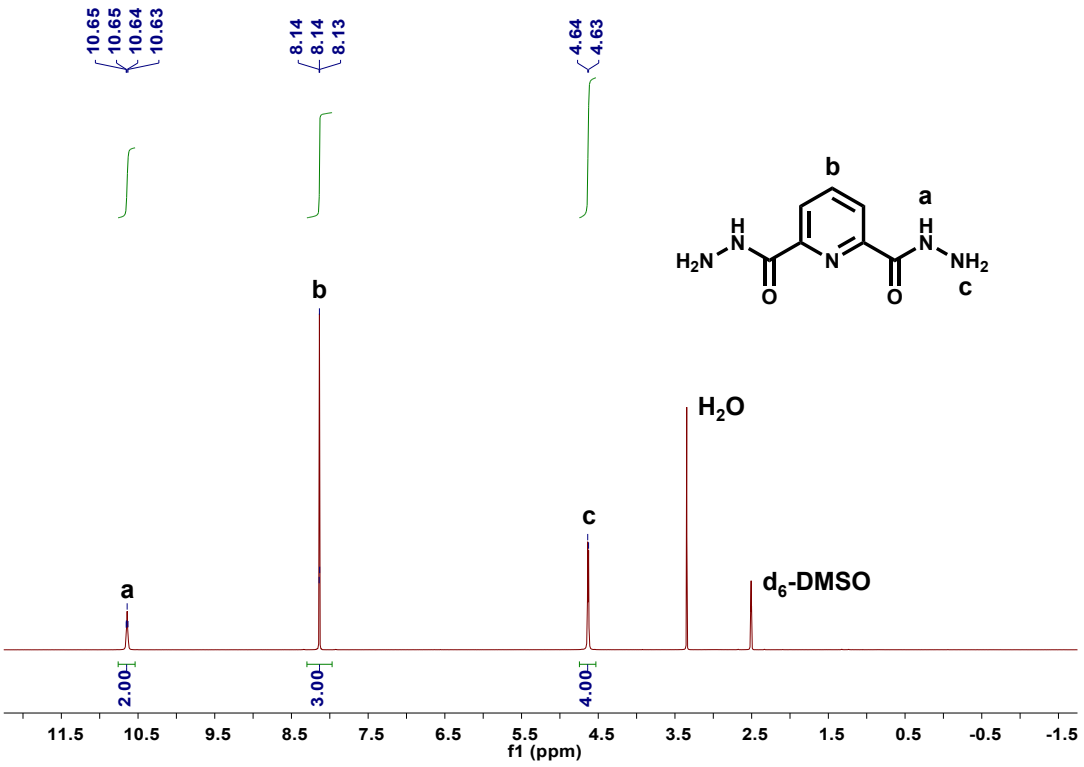

Fig. S14 [1]H NMR spectrum of PDCH.

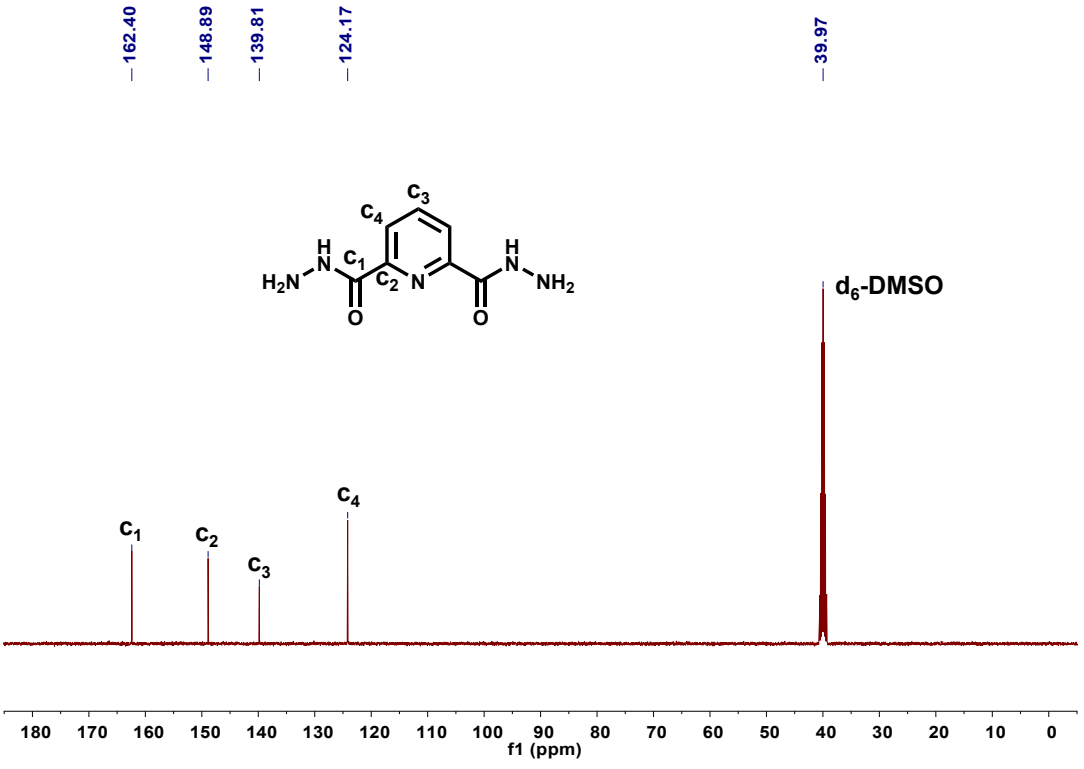

Fig. S15 [13]C NMR spectrum of PDCH.

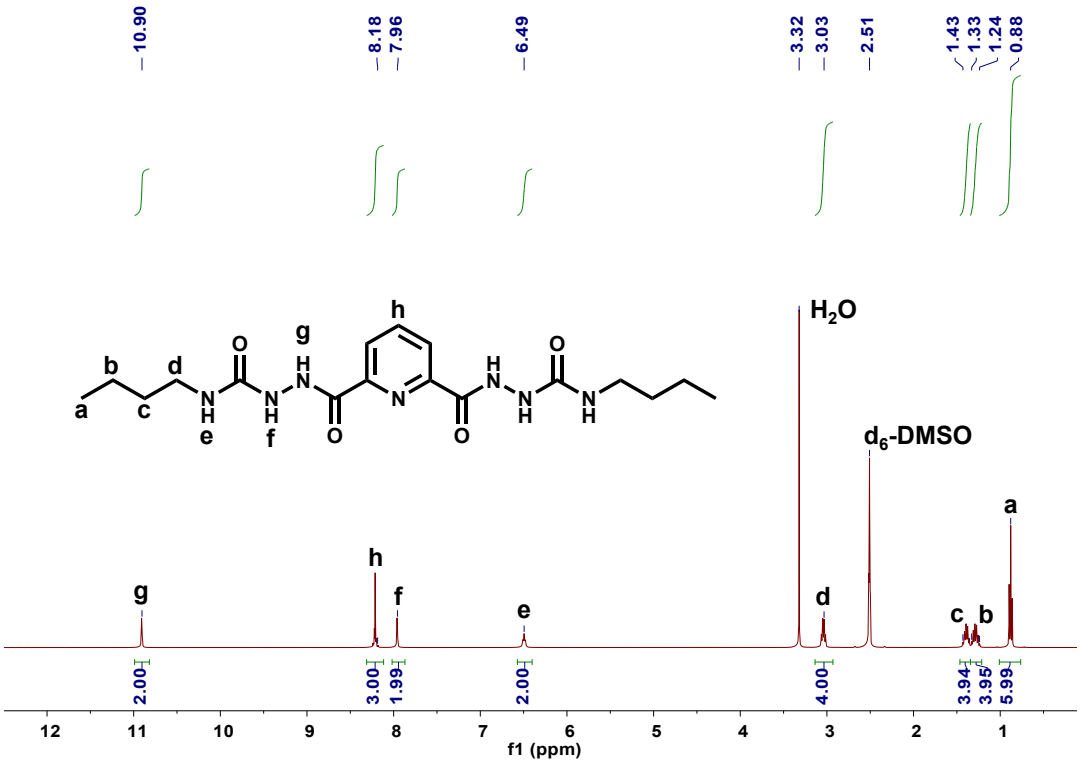

Fig. S16 ^{1}H NMR spectrum of BI-PDCH-BI.

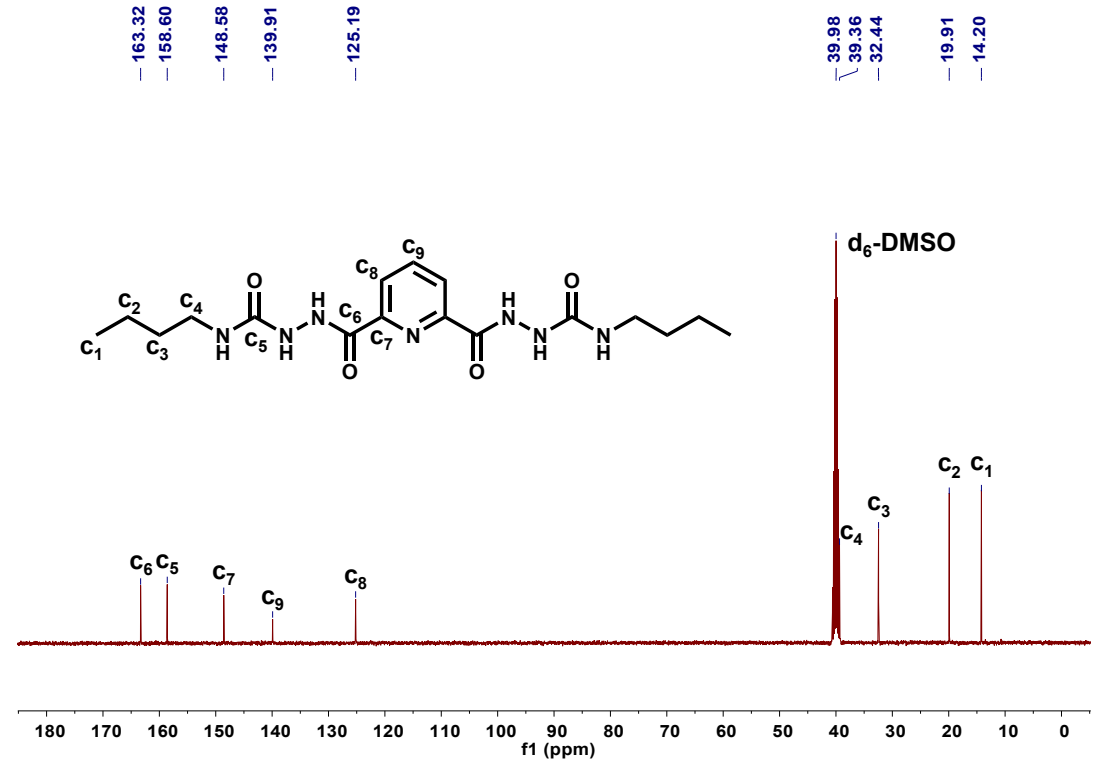

Fig. S17 ^{13}C NMR spectrum of BI-PDCH-BI.

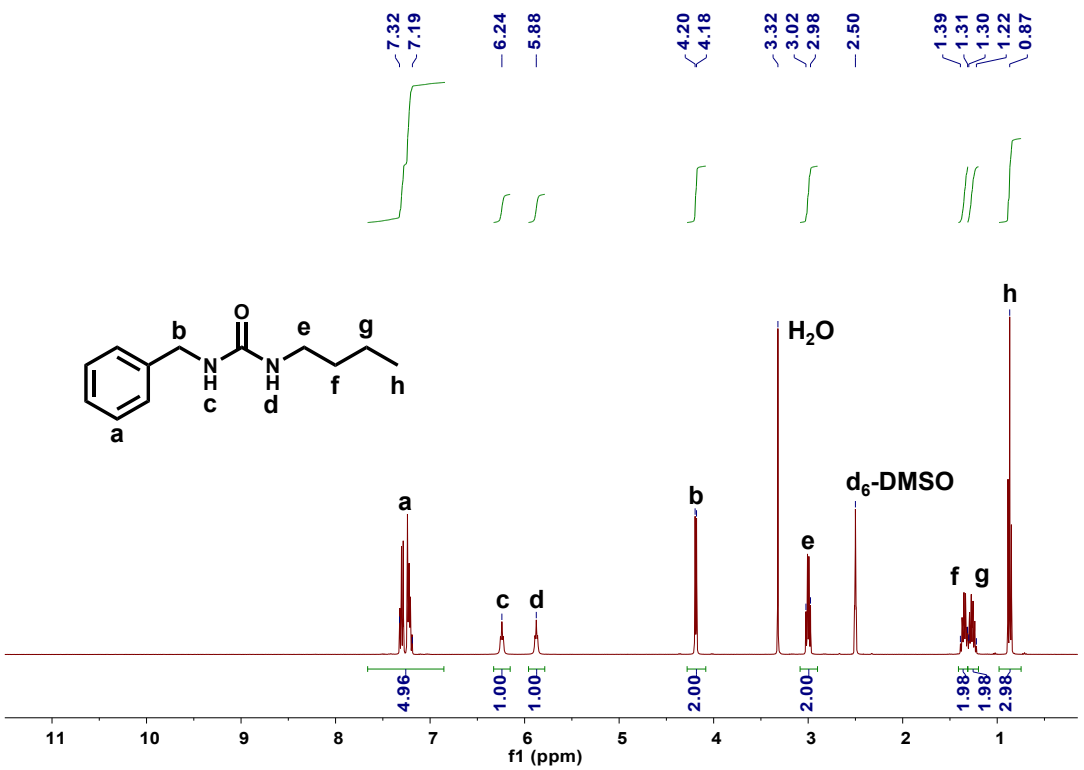

Fig. S18 ^{1}H NMR spectrum of BA-BI.

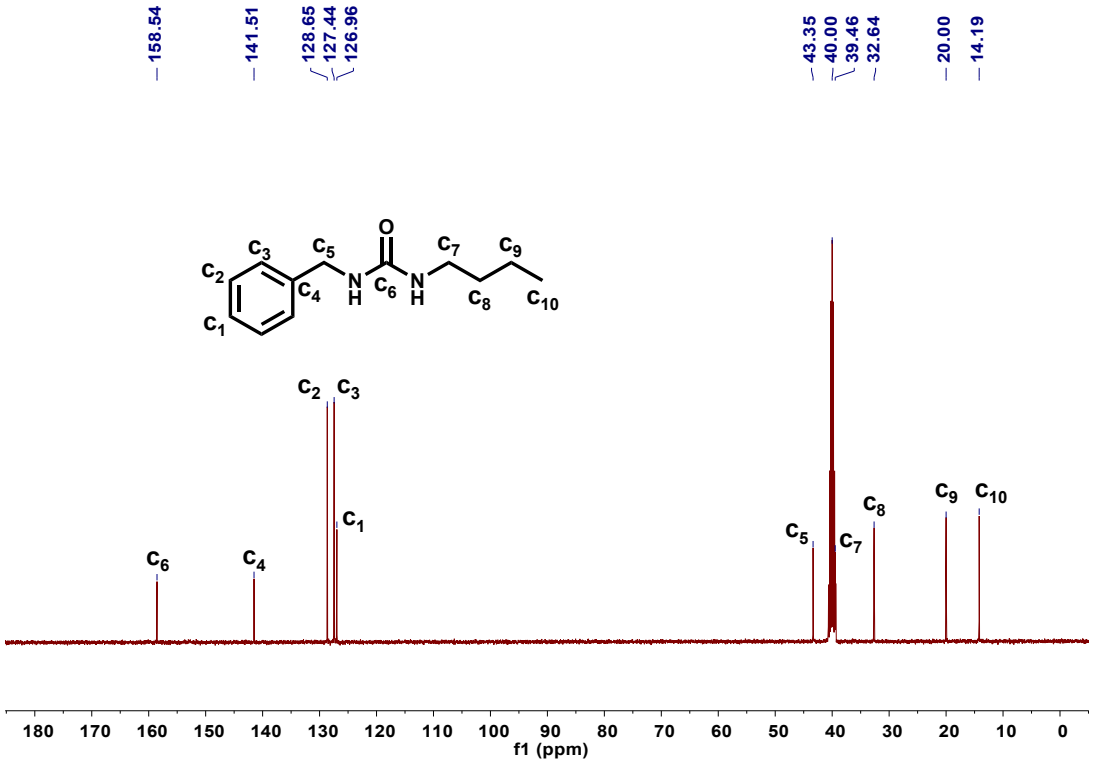

Fig. S19 ^{13}C NMR spectrum of BA-BI.

3. Supplementary Tables

Table S1. The assignments of FTIR bands.

Wavenumber (cm^{-1})	Assignments
3398	*v* (N-H, free), N-H stretching of "free" N-H groups
3347	*v* (N-H, disordered bonded), N-H stretching of disordered hydrogen-bonded N-H groups
3272	*v* (N-H, ordered bonded), N-H stretching of ordered hydrogen-bonded N-H groups
1710	*v* (C=O, free), C=O stretching of "free" C=O groups, amide I
1667	*v* (C=O, disordered bonded), C=O stretching of disordered hydrogen-bonded C=O groups, amide I
1635	*v* (C=O, ordered bonded), C=O stretching of ordered hydrogen-bonded C=O groups, amide I
1625	*v* (C=O, complexation), C=O stretching of coordination-bonded C=O groups, amide I
1568	*δ* (N-H, bonded), N-H bending of hydrogen-bonded N-H groups, amide II
1546	*δ* (N-H, free), N-H bending of "free" N-H groups, amide II
1517	*v* (C-N=C, free), C-N=C stretching of pyridine rings
1508	*v* (C-N=C, complexation), C-N=C stretching of coordinated pyridine rings
1106	*v* (C-O-C), C-O-C stretching vibration band

Table S2. The signs of the cross correlation peaks (v_1, v_2) in synchronous and asynchronous spectra.

Cross correlation peak (cm^{-1}, cm^{-1})	Sign in synchronous spectra	Sign in asynchronous spectra	Sequential order
(3347, 3272)	−	+	3347 ← 3272
(3347, 1667)	−	−	3347 → 1667
(3347, 1635)	−	+	3347 ← 1635
(3347, 1625)	−	+	3347 ← 1625
(3347, 1508)	+	−	3347 ← 1508
(3347, 1106)	−	+	3347 ← 1106
(3272, 1667)	+	+	3272 → 1667
(3272, 1635)	+	−	3247 ← 1635
(3272, 1625)	+	−	3247 ← 1625
(3272, 1508)	−	+	3247 ← 1508
(3272, 1106)	+	−	3247 ← 1106
(1667, 1635)	+	−	1667 ← 1635
(1667, 1625)	+	−	1667 ← 1625

(1635, 1625)	+	—	1635 ← 1625□ □□□□□
(1667, 1508)	—	+	1667 ← 1508□ □□□□□
(1667, 1106)	+	—	1667 ← 1106
(1635, 1508)	—	—	1635 → 1508
(1635, 1106)	+	+	1635 → 1106
(1625, 1508)	—	—	1625 → 1508
(1625, 1106)	+	+	1625 → 1106
(1508, 1106)	—	+	1508 ← 1106□ □□□□□

Table S3. Mechanical properties of the crosslinked PU.

PU	Molar ratio[a]	Young's Modulus (E, MPa)	Stress at Break (σ_b, MPa)	Strain at Break (ε_b, %)	Tensile Toughness (U_T, MJ m^{-3})
PDCH-ASC-PU	9 : 3 : 10.8 : 0.8	187.3 ± 11.5	63.7 ± 1.3	504 ± 12	170.6 ±7.7
Zn-PDCH-ASC-PU-0.25	9 : 3 : 10.8 : 0.8 : 0.75	345.2 ± 6.7	70.7 ± 2.6	549 ± 18	215.1 ± 12.8
Zn-PDCH-ASC-PU-0.5	9 : 3 : 10.8 : 0.8 : 1.5	469.6 ± 17.9	73.6 ± 2.7	511 ± 16	218.2 ± 11.8
Zn-PDCH-ASC-PU-1	9 : 3 : 10.8 : 0.8 : 3	797.4 ± 20.1	67.6 ± 1.1	401 ± 12	172.3 ± 8.1

[a] The molar ratio of ED600 : PDCH : IPDI : tri-HDI : $ZnCl_2$

Table S4. The comprehensive healing and recycling performances of PDCH-ASC-PU.

PDCH-ASC-PU	Samples	Young's Modulus (E, MPa)	Stress at Break (σ_b, MPa)	Strain at Break (ε_b, %)	Tensile Toughness (U_T, MJ m^{-3})	Recovery Efficiency[a] (%)
Healing	110 ℃, 5 min	177.1 ± 4.8	14.7 ± 0.8	51 ± 2	6.7 ± 0.3	~3.9
	110 ℃, 1 h	171.7 ± 9.3	21.4 ± 1.1	156 ± 5	24.8 ± 1.1	~14.5
	110 ℃, 3 h	167.1 ± 15.2	35.1 ± 1.6	286 ± 8	62.4 ± 2.8	~36.6
	110 ℃, 6 h	167.8± 13.7	40.0 ± 0.5	322 ± 6	73.9 ± 2.4	~43.3
	110 ℃, 12 h	165.1 ± 6.9	41.9 ± 1.7	339 ± 9	82.3 ± 3.8	~48.2
Recycling[b]	110 ℃, 1h	185.6 ± 7.6	33.6 ± 0.9	280 ± 5	58.9 ± 1.7	~34.5
	120 ℃, 1h	177.1 ± 6.6	50.9 ± 1.7	416 ± 8	113.3 ± 4.1	~66.4
	140 ℃, 1h	168.8 ± 4.2	62.7 ± 2.1	529± 13	171.9 ± 8.2	~100.8
	130 ℃, 10 min	180.7 ± 8.6	27.6 ± 1.2	208 ± 6	39.3 ± 1.7	~23.0
	130 ℃, 30 min	176.5 ± 7.3	49.1 ± 2.8	413 ± 8	114.3 ± 3.9	~67.0
	130 ℃, 1h[c]	175.1 ± 9.7	65.3 ± 2.4	525 ± 14	178.7 ± 9.1	~104.7
	2nd generation	171.7 ± 11.2	61.6 ± 1.9	509 ± 12	166.3 ± 7.4	~94.5
	3rd generation	166.2 ± 6.5	58.6 ± 1.6	485 ± 10	149.3 ± 5.9	~87.5

[a] The recovery efficiency is the toughness of healed/recycled sample over that of the intrinsic sample (Tables S3). [b] Hot-pressing at different temperature for different durations of time under a pressure of 10 MPa. [c] Hot-pressing at 130 ℃ for 1h is the recycling condition for 1st generation sample.

Table S5. The comprehensive healing and recycling performances of PDCH-ASC-PU-0.5.

Zn-PDCH-ASC-PU-0.5	Samples	Young's Modulus (E, MPa)	Stress at Break (σ_b, MPa)	Strain at Break (ε_b, %)	Tensile Toughness (U_T, MJ m^{-3})	Recovery Efficiency[a] (%)
Healing	110 ℃, 5 min	440.0 ± 11.4	30.3 ± 0.9	164 ± 5	38.0 ± 1.5	~17.4
	110 ℃, 1 h	446.6 ± 9.8	51.0 ± 1.3	337 ± 8	107.9 ± 4.1	~49.5
	110 ℃, 3 h	461.2 ± 15.6	60.8 ± 1.1	414 ± 7	148.3 ± 4.3	~68.0
	110 ℃, 6 h	447.6 ± 8.7	68.5 ± 1.9	469 ± 9	185.9 ± 6.2	~85.2
	110 ℃, 12 h	436.4 ± 6.3	70.2 ± 2.5	484 ± 5	195.4 ± 3.5	~89.6
Recycling[b]	130 ℃, 10 min	470.4 ± 4.3	52.1 ± 2.8	373 ± 4	123.8 ± 2.1	~56.7
	130 ℃, 30 min	436.4 ± 8.7	71.2 ± 2.4	500 ± 8	201.9 ± 5.7	~92.5
	130 ℃, 1h[c]	418.0 ± 6.8	74.4 ± 2.1	531 ± 7	220.3 ± 5.2	~100.9
	2nd generation	393.4 ± 5.9	71.0 ± 2.6	516 ± 12	209.0 ± 8.5	~95.8
	3rd generation	383.1 ± 9.2	69.4 ± 2.7	491 ± 11	189.6 ± 7.6	~86.9

[a] The recovery efficiency is the toughness of healed/recycled sample over that of the intrinsic sample (Tables S3). [b] Hot-pressing at different temperature for different durations of time under a pressure of 10 MPa. [c] Hot-pressing at 130 ℃ for 1h is the recycling condition for 1st generation sample.

Table S6. The comprehensive healing performances of Zn-PDCH-ASC-PU-0.25.

Zn-PDCH-ASC-PU-0.25	Samples	Young's Modulus (E, MPa)	Stress at Break (σ_b, MPa)	Strain at Break (ε_b, %)	Tensile Toughness (U_T, MJ m^{-3})	Recovery Efficiency[a] (%)
Healing	110 ℃, 5 min	347.3 ± 9.5	21.5 ± 0.5	113 ± 4	20.1 ± 0.9	~9.3
	110 ℃, 1 h	333.4 ± 7.8	40.6 ±1.2	309 ± 9	79.1 ± 3.7	~36.8
	110 ℃, 3 h	343.7 ± 6.5	52.2 ± 2.3	395 ± 6	120.3 ± 3.1	~55.9
	110 ℃, 6 h	340.3 ± 8.9	59.7 ± 1.6	453 ± 8	152.1 ± 4.8	~70.7
	110 ℃, 12 h	353.5 ± 7.3	61.8 ± 2.1	469 ± 9	163.5 ± 5.6	~76.0

[a] The recovery efficiency is the toughness of healed/recycled sample over that of the intrinsic sample (Tables S3).

Table S7. The comprehensive healing performances of Zn-PDCH-ASC-PU-1.

Zn-PDCH-ASC-PU-1	Samples	Young's Modulus (E, MPa)	Stress at Break (σ_b, MPa)	Strain at Break (ε_b, %)	Tensile Toughness (U_T, MJ m^{-3})	Recovery Efficiency[a] (%)
Healing	110 ℃, 5 min	786.0 ± 11.8	31.5 ± 0.6	105 ± 6	30.4 ± 1.9	~17.6
	110 ℃, 1 h	788.3 ± 10.5	44.7 ± 1.2	241 ± 8	81.5 ± 3.6	~47.3
	110 ℃, 3 h	746.2 ± 9.6	56.4 ± 0.9	321 ± 8	120.7 ± 4.5	~70.1
	110 ℃, 6 h	749.0 ± 12.4	61.9 ± 2.5	361 ± 7	143.2 ± 4.3	~83.1
	110 ℃, 12 h	744.6 ± 14.3	64.1 ± 1.7	381 ± 9	154.0 ± 5.8	~89.4

[a] The recovery efficiency is the toughness of healed/recycled sample over that of the intrinsic sample (Tables S3).

4. Supplementary movies

Movie S1. Self-healing behaviour of PDCH-ASC-PU.

Movie S2. Self-healing behaviour of Zn-PDCH-ASC-PU-0.5.

5. Supplementary References

1 D. J. Skrovanek, P. C. Painter, M. M. Coleman, *Macromolecules*, 1986, **19**, 699-705.
2 G. Rusu, K. Ueda, E. Rusu, M. Rusu, *Polymer*, 2001, **42**, 5669-5678.
3 Y. Song, H. Yamamoto, N. Nemoto, *Macromolecules*, 2004, **37**, 6219-6226.
4 C.-H. Li, C. Wang, C. Keplinger, J.-L. Zuo, L. Jin, Y. Sun, P. Zheng, Y. Cao, F. Lissel, C. Linder, X.-Z. You, Z. Bao, *Nat. Chem.*, 2016, **8**, 619-625.